Effect of the Donor−Bridge Energy Gap on the Electron-Transfer Mechanism in Donor−Bridge−Acceptor Systems

ARTICLE *in* THE JOURNAL OF PHYSICAL CHEMISTRY B · JULY 2005

Impact Factor: 3.3 · DOI: 10.1021/jp0503112 · Source: PubMed

1 AUTHOR:

Eunji Sim
Yonsei University
62 PUBLICATIONS **847** CITATIONS

SEE PROFILE

Effect of the Donor−Bridge Energy Gap on the Electron-Transfer Mechanism in Donor−Bridge−Acceptor Systems

Eunji Sim*

Department of Chemistry, Yonsei University, 134 Sinchondong Seodaemungu, Seoul 120-749, South Korea

Received: January 18, 2005; In Final Form: March 24, 2005

The effect of the energy gap between donor and bridge states in the electron transfer of a double mutant photosynthetic purple bacterial reaction center is thoroughly investigated using a recently introduced modified on-the-fly filtered propagator important path integral formalism. By decomposition of the reduced density matrix of a system coupled to a dissipative environment, partial contributions of incoherent hopping, coherent superexchange, and partially coherent hopping transport to the overall electron or charge transfer are evaluated. Within the tight-binding donor−bridge−acceptor model, the three mechanisms coexist for a wide range of donor−bridge energy gap values, and the governing mechanism changes from incoherent hopping to partially coherent hopping and eventually to coherent superexchange as the donor−bridge energy gap becomes large.

1. Introduction

Designing and developing effective molecular electronic devices and polymeric electron-transfer materials depends on understanding details of the electron-transfer mechanism.[1−3] In the case of long-range bridge-mediated molecular systems, for instance, it has been well-known that incoherent hopping leads to more efficient electron transfer than coherent superexchange does. The transfer rate of coherent superexchange exponentially decreases with the distance between states while the transfer rate of incoherent hopping is more or less independent of the distance.[4−7] What determines the electron-transfer mechanism and in what condition incoherent hopping governs the transport are still arguments to be resolved. In general, coherent superexchange and incoherent hopping were regarded as alternatives in the electron-transfer mechanism. Only recently, however, it was revealed that incoherent hopping and coherent superexchange may both be present in a single system, rather than preclude each other, with a varying degree of respective contribution to the overall electron or charge transfer.[8−10] In particular, coherent superexchange does not dominate the transport in all configurations whose bridge-state energy is higher than the donor-state energy. The incoherent hopping pathway may also contribute significantly to the electron transfer in such configurations, despite the fact that it is unfavorable to make an upward jump to a bridge state from a low-lying donor state.[8]

To understand details of the electron-transfer mechanism, the relative transfer efficiency from different mechanisms should be available. Two types of electron-transfer mechanisms typically have been explored, incoherent hopping and coherent superexchange. In this article, the electron-transfer mechanism is classified into three groups including partially coherent hopping transport. In a coherent superexchange pathway, electrons take a direct route from a donor to an acceptor or from an acceptor to a donor no matter how many bridges may exist between the two states. On the contrary, for an incoherent hopping pathway, electrons must hop from one site to its nearest neighbors. Upon close examination, one can see that electrons can also make incoherent hopping and coherent superexchange migrations between states in a single path, hence a partially coherent hopping pathway. Determination of the relative transfer efficiency of each of the three mechanisms requires separating one mechanism from the rest and isolating the contribution of an individual mechanism to the electron transfer. There have been studies to estimate the relative contribution of both coherent and incoherent hopping to the overall transport in a conjugated bridge molecule.[9,10] Petrov et al. described nonadiabatic bridge-assisted donor−acceptor electron transfer with single-exponential kinetics and evaluated the relative ratio of incoherent hopping and coherent superexchange transfer rates to stand for the relative transfer efficiency of the two mechanisms.[9] However, Weiss and co-workers obtained the probability of the coherent electron-transfer mechanism spectroscopically.[10] Only the relative magnitudes of the two mechanisms were considered in the study, where the possibility of the partially coherent hopping mechanism was ignored. To study the electron-transfer mechanism, it is necessary to obtain not only the relative magnitude of the contribution but also the absolute amount of electrons transferred through each mechanism. More importantly, partially coherent hopping pathways should be examined as an intermediate between incoherent hopping and coherent superexchange. In recent publications, we introduced a modified on-the-fly filtered propagator functional (OFPF) important path integral method, in which the reduced density matrix of the system is decomposed into partial density matrices of incoherent hopping, coherent superexchange, and partially coherent hopping.[8,11] Since the contribution of one mechanism to the density matrix in the path integration is independent of the others, it is possible to calculate not only the relative transfer efficiency of each mechanism but also the absolute amount of transported electronic charge population changes over the time. This provides an extremely efficient and useful tool to thoroughly investigate the electron-transfer mechanism.

Among many important issues, the effects of potential parameters on the electron-transfer mechanism need to be particularly clarified. Various parameters, such as the energy gap, electronic coupling between states, and solvent reorganiza-

* Author to whom correspondence should be addressed. Fax: +82-2-364-7050. E-mail: esim@yonsei.ac.kr.

10.1021/jp0503112 CCC: $30.25
Published on Web 05/18/2005

tion energy, play crucial roles in determining the governing electron-transfer mechanism.[12] However, the impact of an individual parameter on the transport remains elusive. The electronic coupling between a donor and a bridge controls the decay of electronic accumulation in the donor state. In contrast, the electronic coupling between a bridge and an acceptor affects the charge accumulation in a bridge state. For distant donors and acceptors, a donor and an acceptor interact with an effective superexchange coupling constant that arises from virtual bridges between the donor and the acceptor. The McConnell product of the form that depends on electronic coupling constants between nearest-neighbor states and the energy gap can estimate the effective superexchange coupling constant.[12,13] Yet it is unclear how these parameters determine the dominant type of overall transfer mechanism.

The article is organized as follows. In section 2, we explain a real-time quantum mechanical simulation method in which pathways belonging to an electron-transfer mechanism are separated and integrated independently from the other pathways. In section 3, the time evolution of the electronic population of a double mutant photosynthetic purple bacterial reaction center at various donor−bridge energy gaps is evaluated. To explore the relative transfer efficiency of each mechanism, a net flux ratio is defined and evaluated as a function of the donor−bridge energy gap while electronic coupling between the states and the donor−acceptor energy gap are kept constant. On the basis of the numerical results, the electron-transfer mechanism is analyzed, and the role of the donor−bridge energy gap is discussed. Concluding remarks appear in section 4.

2. Methodology

In this section, we examine a real-time quantum mechanical simulation method that is based on Feynman and Vernon's influence functional path integral approach on a system coupled to baths.[14−16] Within the tight-binding system−bath Hamiltonian model,[17] a system is represented in terms of M discrete electronic sites involved in electronic transport, reduced electronic states of a donor, bridges, and an acceptor. While the bath consists of Q explicit modes, either harmonic or anharmonic, weak interaction between the system and the bath is assumed within the linear response limit.[18] The Hamiltonian is written as

$$H = \sum_{k=1}^{M}\sum_{k'=1}^{M} h_{kk'}|k\rangle\langle k'| + H_{\mathrm{b}}(\mathbf{x}) - \sum_{n=1}^{Q} c_n x_n \sum_{k=1}^{M} \tilde{s}_k |k\rangle\langle k| \tag{1}$$

where $|k\rangle$ denotes the kth electronic site located at $\tilde{s}_k$. The first two terms are, respectively, the bare system and the bath Hamiltonian. x_n is an nth bath mode coordinate that is coupled to the system with a coupling constant c_n. Bath properties relevant to the dynamics of the system are contained in the spectral density that includes the solvent polarization. For this work, an ohmic form of the spectral density has been chosen[17]

$$J(\omega) = \frac{\pi\hbar}{2}\xi\omega \exp(-\omega/\omega_{\mathrm{c}}) \tag{2}$$

where ξ is the dimensionless Kondo parameter and ω_{c} is the characteristic cutoff frequency of the bath.

Time evolution of the reduced density matrix, defined as

$$\tilde{\boldsymbol{\rho}}(t) = \mathrm{Tr}_{\mathrm{b}}[\mathrm{e}^{-\mathrm{i}Ht/\hbar}\,\boldsymbol{\rho}(0)\,\mathrm{e}^{\mathrm{i}Ht/\hbar}] \tag{3}$$

is particularly useful for the study of electron transfer, since the diagonal elements express the relaxation over time of the electron population on the three reduced sites. In eq 3, Tr_{b} is the trace with respect to all bath degrees of freedom. $\boldsymbol{\rho}(0)$ is the initial density matrix of the system and the bath in thermal equilibrium and has a factorized form $\boldsymbol{\rho}(0) = \tilde{\boldsymbol{\rho}}(0)\,\mathrm{e}^{-\beta H_{\mathrm{b}}}/Z_{\mathrm{b}}$ with Z_{b} as the bare bath partition function. Performing a trace of the bath degree of freedom is straightforward in the case of the Harmonic oscillator bath, and a closed form of the expression results after Gaussian integrations. For anharmonic baths, a recent development that uses effective harmonic bath modes can be useful, where the spectral density of the effective harmonic bath is evaluated as[18]

$$J_{\mathrm{eff}}(\omega,\beta) = \frac{2}{\hbar}\tanh\left(\frac{1}{2}\hbar\omega\beta\right)\int_0^\infty \mathrm{d}t\ \mathrm{Re}\sum_{n=1}^{Q} {c_n}^2\langle x_n(0)x_n(t)\rangle_\beta \cos\omega t\, J(\omega) \tag{4}$$

with $\langle\cdots\rangle_\beta$ being the equilibrium average with respect to the bare bath.

Following Feynman and Vernon's influence functional formalism and by discretizing paths in time, eq 3 can be written as a multidimensional summation of the product of the system propagator and the influence functional

$$\tilde{\boldsymbol{\rho}}(t) = \sum_{i}^{L_{\mathrm{tot}}} \mathbf{S}(\Gamma_i^{(N)})\,\mathbf{I}(\Gamma_i^{(N)}) \tag{5}$$

where the time is discretized into N time steps of length $\Delta t = t/N$. $\Gamma_i^{(N)}$ is a path segment from time 0 to t that belongs to the ith path. The summation in eq 5 runs over all possible paths connecting donor and acceptor electronic states leading to $L_{\mathrm{tot}} = M^{2N}$.

At this point, we discuss the type of electron-transfer mechanism. For the sake of simplicity, we consider the simplest bridge-mediated electron-transfer system, a donor−bridge−acceptor complex. It is straightforward to extend the discussion to long-distance electron-transfer systems. By taking incoherent hopping pathways, electrons hop from one site to its nearest neighbors, such as donor to bridge, bridge to donor or acceptor, and acceptor to bridge, while electrons take a direct route from (to) a donor to (from) an acceptor in coherent superexchange pathways. Among L_{tot} paths, a mechanism can be identified by collecting pathways that belong to a particular mechanism such as incoherent hopping, coherent superexchange, and partially coherent hopping as well as a static mechanism. The partially coherent hopping includes pathways that make incoherent and coherent jumps between states in a single path. Static pathways, although they do not contribute to the transport, are still possible such that electrons do not leave their initial state. Therefore, the reduced density matrix of the system in eq 3 can be written as a sum of four partial density matrices[8]

$$\tilde{\boldsymbol{\rho}}(t) = \tilde{\boldsymbol{\rho}}^{\mathrm{i}}(t) + \tilde{\boldsymbol{\rho}}^{\mathrm{c}}(t) + \tilde{\boldsymbol{\rho}}^{\mathrm{p}}(t) + \tilde{\boldsymbol{\rho}}^{\mathrm{s}}(t) \tag{6}$$

where the superscript i stands for incoherent hopping, c for coherent superexchange, p for partially coherent hopping, and s for a static mechanism. Through decomposition of the reduced density matrix, it is easy to see that each mechanism contributes to the full density matrix elements and is uncorrelated with the other, allowing independent computation of the partial density matrices. An individual partial density matrix is calculated as eq 5, except that the summation runs only over the pathways that belong to the corresponding mechanism. Notice that the trace of the full reduced density matrix should be unity, i.e.,

$\sum_{i=1}^{M} \tilde{\rho}_{ii} = 1$; however, the trace of each partial density matrix has no such condition.

The OFPF important path integral approach rewrites eq 5 as a sum of the products of the history and propagator functionals[11]

$$\tilde{\boldsymbol{\rho}}^{\chi}(t) = \sum_{i_\chi}^{L_\chi} \mathscr{T}(\Gamma_{i_\chi}^{(N-1)}) \mathscr{P}^{e}(\Gamma_{i_\chi}^{(N)}) \quad \chi = \mathrm{i,c,p,s} \tag{7}$$

where L_χ is the number of paths that belong to χ mechanism and $\Gamma_{i_\chi}^{(l)}$ is the path segment from time 0 to $l\Delta t$ that belongs to the ith pathway of χ mechanism. For the density matrix at the present time t, the history term involves interactions between the past time points (from 0 to $t - \Delta t$)

$$\mathscr{T}(\Gamma_{i_\chi}^{(N-1)}) = \langle k_0^+ | \tilde{\boldsymbol{\rho}}(0) | k_0^- \rangle \prod_{j=1}^{N-1} S_{k_j} \prod_{j=0}^{N-1} \prod_{j'=0}^{j} I_{k_j k_{j'}} \tag{8}$$

while the propagator functional includes the interactions between the present and the past time points

$$\mathscr{P}^{e}(\Gamma_{i_\chi}^{(N)}) = S_{k_N} \prod_{j=0}^{N} I_{k_N k_j} \tag{9}$$

Here, the + (−) sign in the superscripts depicts the forward (backward) propagating path segments. The system propagator **S** accounts the transport within the system in the absence of baths while the influence functional **I** arises from the coupling to the environment such that

$$S_{k_j} = \langle k_j^+ | e^{-iH_s \Delta t/\hbar} | k_{j-1}^+ \rangle \langle k_{j-1}^- | e^{iH_s \Delta t/\hbar} | k_j^- \rangle \tag{10}$$

and

$$I_{k_j k_{j'}} = \exp\left\{ -\frac{1}{\hbar} (\tilde{s}_{k_j^+} - \tilde{s}_{k_j^-}) (\eta_{k_j k_{j'}} \tilde{s}_{k_{j'}^+} - \eta_{k_j k_{j'}}^* \tilde{s}_{k_{j'}^-}) \right\} \tag{11}$$

where $\tilde{s}_{k^+}$ ($\tilde{s}_{k^-}$) corresponds a grid point at time $j\Delta t$ in the kth forward (backward) path and expressions for the influence coefficients $\eta_{kk'}$ that can be found in ref 19.

By identifying the history and the propagator functional terms and by saving the weight of the history path segments, a significant amount of redundant calculations are avoided. Nevertheless, as one propagates, the number of configurations and corresponding weights to be stored increases exponentially as M^{2N}. As the strength of nonlocal interactions due to dissipative baths drops off rapidly beyond a certain value of $\tau_m = N_m \Delta t$, it is sufficient to include only M^{2N_m} configurations for the times $t > \tau_m$ without losing numerical accuracy, leading to the saturation of the number of paths to be included in the path integration.[15] In addition, in each propagation step, the OFPF important path integration performs on-the-fly filtering such that, up to $t = \tau_m$, the number of paths increases linearly with the propagation time.

3. Discussion

The path integral formalism discussed in section 2 is applicable to electron-transfer systems with any number of electronic sites. In this section, we restrict our discussion to the simplest bridge-mediated electron-transfer systems, i.e., a donor−bridge−acceptor system, in particular, the double mutant of the photosynthetic purple bacterial reaction center by Heller et al.[20] The wild-type of the bacterial reaction center takes a bacteriochlorophyll special pair as a donor, bacteriochlorophyll as a bridge, and bacteriopheophytin as an acceptor. The wild-type exhibits an incoherent hopping transfer mechanism with the bridge-state energy lower than that of the donor. However, both the bridge and acceptor of the double mutant are mutated from the wild-type such that bacteriochlorophyll is the bridge and bacteriopheophytin with a substituted aspartic acid is the acceptor. The double mutant is known to have a bridge-state energy higher than the donor-state energy.[21,22] Therefore, the electron transfer in the double mutant has been generally considered to be governed by the coherent superexchange mechanism. Recently, however, it was found that the electron transfer within the double mutant is dominated by the incoherent hopping mechanism despite the high-energy bridge state.[8] In this section, the effect of the donor−bridge energy gap on the electron transfer in the double mutant is explored.

To model the double mutant of the purple bacterial reaction center, the system Hamiltonian in eq 1 has a 3×3 matrix form

$$\mathbf{H}_s = \begin{pmatrix} 0 & V_{12} & 0 \\ V_{12} & E_2 & V_{23} \\ 0 & V_{23} & E_3 \end{pmatrix} \tag{12}$$

where the parameters are chosen to be $V_{12} = 22\ \mathrm{cm}^{-1}$, $V_{23} = 135\ \mathrm{cm}^{-1}$, and $E_3 = -400\ \mathrm{cm}^{-1}$. The system−bath interaction is described by the Ohmic spectral density with a characteristic frequency of $\omega_c = 600\ \mathrm{cm}^{-1}$ and the Kondo parameter $\xi = 1.67$. With $E_2 = 500\ \mathrm{cm}^{-1}$, this particular set of parameters corresponds to the double mutant of the reaction center discussed in Heller et al.[20−22] Note that the direct electronic coupling between donor and acceptor states is set to be zero such that the direct donor-to-acceptor transport can occur only by way of a virtual bridge that provides effective coupling between the two states without electrons ever populating the bridge. It is assumed that the system is initially in the donor state and the distances between nearest states are equal. Room temperature is applied for all of the simulations presented in this article. In the remainder of the article, energies are written in terms of the thermal energy $\beta^{-1} = k_B T$ to implicitly represent the change in the thermally activated population with respect to the donor−bridge energy gap.

Three diagonal elements ($\tilde{\rho}_{11}$ for the donor, $\tilde{\rho}_{22}$ for the bridge, and $\tilde{\rho}_{33}$ for the acceptor) of the reduced density matrix denote the charge population on the corresponding state and well present the decay and increase in the charge population throughout the transport. In Figure 1, the decay of $\tilde{\rho}_{11}$ over time is equivalent to the charge migration from the donor to the bridge and acceptor while the rise of $\tilde{\rho}_{33}$ depicts the charge accumulation and trapping in the acceptor. With $\beta E_2 = 3$, the electron accumulation in the bridge state is less than 5% throughout the transport. Without comparison of the full density matrix with the incoherent hopping partial density matrix, the overall electron transfer seems to be due to the coherent superexchange. In Figure 1, the full density matrix and the incoherent hopping partial density matrix show excellent agreement, which indicates that the incoherent hopping is in fact responsible for the electron transfer. Furthermore, while electrons reside on the bridge through incoherent hopping migrations, it may be difficult to detect the electronic population in the bridge state if electrons hop to an acceptor state as soon as the electronic accumulation occurs on the bridge.[8] Strong coupling between the bridge and acceptor induces rapid transfer between the two states; thus, no or negligible charge accumulation on the bridge is observed. The share of the coherent superexchange to the rise of the acceptor population is also examined and is insignificant in Figure 1.

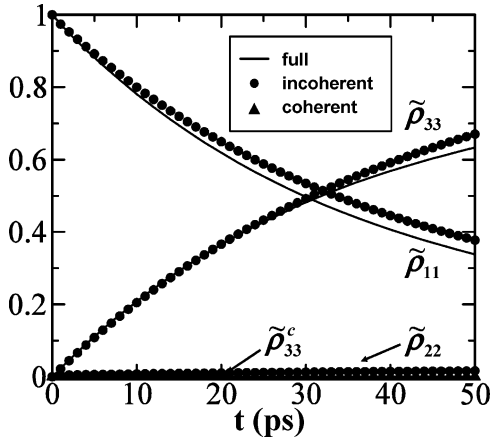

Figure 1. Three diagonal elements of the reduced density matrix ($\tilde{\rho}_{11}$ for the donor, $\tilde{\rho}_{22}$ for the bridge, and $\tilde{\rho}_{33}$ for the acceptor) with $E_2 = 3\beta^{-1}$ obtained by including all pathways $\tilde{\boldsymbol{\rho}}(t)$ (solid lines), by only including incoherent hopping pathways $\tilde{\boldsymbol{\rho}}^{i}(t)$ (circles), and by only including coherent superexchange pathways $\tilde{\boldsymbol{\rho}}^{c}(t)$ (triangles). $\tilde{\boldsymbol{\rho}}(t)$ and $\tilde{\boldsymbol{\rho}}^{i}(t)$ display agreement, and $\tilde{\rho}^{c}_{33}(t)$ is negligible.

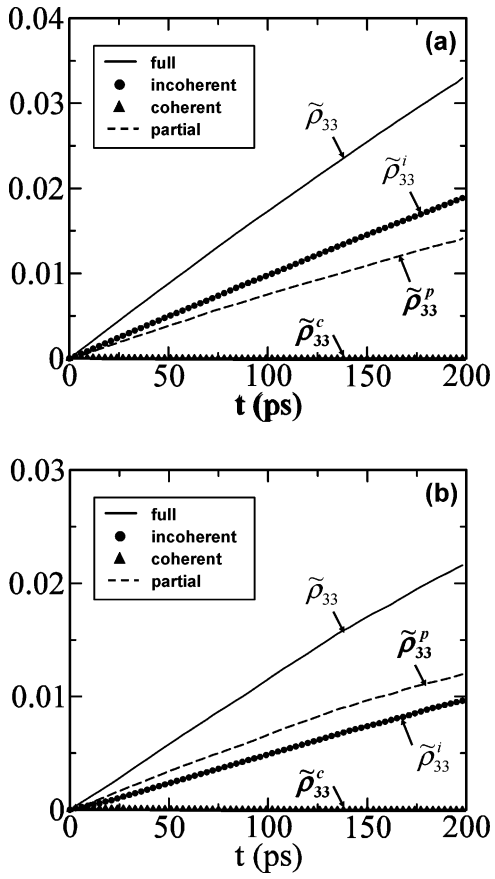

Figure 2. Time evolution of the acceptor electron accumulation $\tilde{\rho}_{33}$ with (a) $E_2 = 20\beta^{-1}$ and (b) $E_2 = 25\beta^{-1}$ obtained by including all pathways $\tilde{\boldsymbol{\rho}}(t)$ (solid lines), by only including incoherent hopping pathways $\tilde{\boldsymbol{\rho}}^{i}(t)$ (circles), by only including coherent superexchange pathways $\tilde{\boldsymbol{\rho}}^{c}(t)$ (triangles), and by only including partially coherent hopping pathways $\tilde{\boldsymbol{\rho}}^{p}(t)$. Note that the coherent superexchange contribution is negligible.

As the bridge-state energy is increased, i.e., the donor−bridge energy gap becomes large, hoppings from donor to bridge are less favorable, and tunneling to the acceptor, i.e., coherent superexchange migrations, is more accessible. In Figures 2a and 2b, where $\beta E_2 = 20$ and 25, respectively, incoherent hopping and partially coherent hopping transfer almost equal amounts of charges to the acceptor. While the difference between $\tilde{\rho}^{i}_{33}$ and $\tilde{\rho}^{p}_{33}$ is not large, nevertheless the contribution of the incoherent hopping $\tilde{\rho}^{i}_{33}$ is slightly larger than that of the partially coherent hopping one $\tilde{\rho}^{p}_{33}$ in the case of $\beta E_2 = 20$. Where $\beta E_2 = 25$, the relative magnitudes of the incoherent hopping and partially coherent hopping pathway are reversed such that $\tilde{\rho}^{p}_{33} > \tilde{\rho}^{i}_{33}$. Figures 2a and 2b demonstrate that if the energy gap is as large as $\beta E_2 = 20$ and 25, then the incoherent hopping is no longer the sole governing electron-transfer mechanism. While both the incoherent hopping and partially coherent hopping participate in the electron transfer from $\beta E_2 = 3$ and $\beta E_2 = 20$, the charge population transported by the incoherent hopping is larger than that by the partially coherent hopping. As the bridge-state energy is increased over $\beta E_2 = 20$, electrons prefer partially coherent hopping pathways to incoherent hopping ones. It indicates that, for an energy gap that is too large for electrons to overcome by taking incoherent hopping pathways, electrons migrate through an intermediate mechanism in the form of the partially coherent hopping pathways in which incoherent hopping and coherent superexchange tunneling coexist. Notice that, with a large energy gap of $\beta E_2 = 20-25$, pure coherent superexchange pathways are not yet actively involved in the electron transfer such that the purely coherent superexchange density matrix element $\tilde{\rho}^{c}_{33}$ reveals almost no population in both Figures 2a and 2b.

To evaluate the relative transfer efficiency and to determine the dominance of the mechanism, a net flux ratio is defined as $\boldsymbol{\gamma}^{\chi} = \tilde{\boldsymbol{\rho}}^{\chi}/(\tilde{\boldsymbol{\rho}} - \tilde{\boldsymbol{\rho}}^{s})$ with χ being i, c, and p. Considering that the static paths do not transfer charges, the following sum rule is obtained by subtracting the static partial density matrix from eq 6 and by dividing the resulting equation by $(\tilde{\boldsymbol{\rho}} - \tilde{\boldsymbol{\rho}}^{s})$

$$\boldsymbol{\gamma}^{i}(t) + \boldsymbol{\gamma}^{c}(t) + \boldsymbol{\gamma}^{p}(t) = \mathbf{1} \tag{13}$$

such that the sum of the net flux ratios of the incoherent hopping, coherent superexchange, and partially coherent hopping should be equal to unity. The magnitude of the net flux ratios stands for the relative transfer efficiency of the corresponding mechanism. It is important to note that, unlike the diagonal elements of the full density matrix, those of the partial density matrices may have a negative sign. Therefore, net flux ratios may also have negative values, and the sign of a net flux ratio indicates the direction of the electron transfer; through corresponding pathways, a positive ratio means that charges are accumulated in the state while a negative ratio means that charges are removed from the state.

Figure 3 presents the net flux ratios over time at various donor−bridge energy gaps. As a reference configuration, Figure 3a corresponds to a double mutant reaction center where the incoherent hopping governs the electron transfer. The net flux ratio of the incoherent hopping is equal to unity throughout the transfer, and those of the partially coherent hopping and coherent superexchange are close to zero. As the donor−bridge energy gap becomes large, the incoherent hopping net flux ratio decreases while the partially coherent hopping net flux ratio increases. Figures 3c and 3d establish the validity of the change of the most contributed mechanism from incoherent hopping to partially coherent hopping. This result agrees with Figure 2. Coherent superexchange pathways do not participate in the electron transfer if $\beta E_2 = 2.4$ in Figure 3a. With a large energy gap, while overall effect of the coherent superexchange is insignificant, initially there is a noticeable amount of γ^{c}_{33} and γ^{p}_{33} increases as γ^{c}_{33} decreases. In the first 25 ps of Figure 3b,

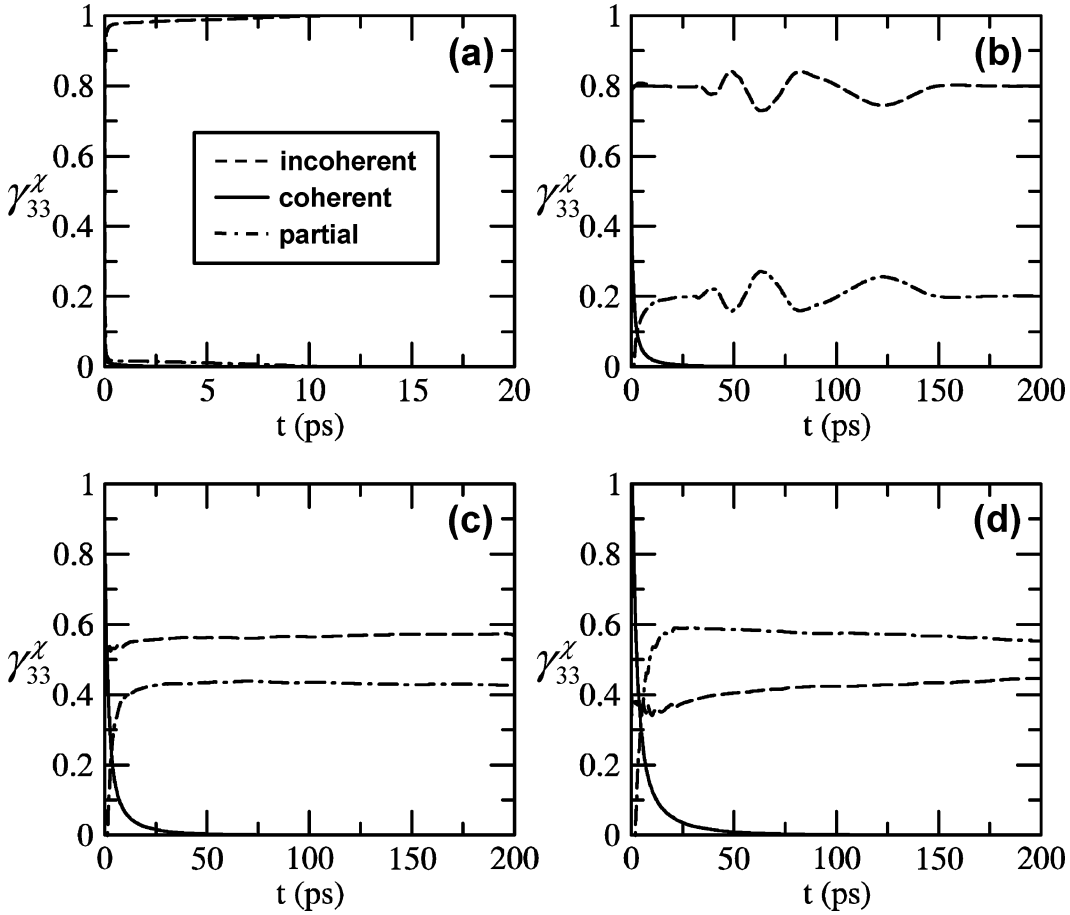

Figure 3. Time evolution of the net flux ratio of the charge accumulation in the acceptor with the energy gap between the donor and the bridge: (a) $E_2 = 2.4\beta^{-1}$, (b) $E_2 = 7\beta^{-1}$, (c) $E_2 = 20\beta^{-1}$, and (d) $E_2 = 25\beta^{-1}$. Dashed lines correspond to the incoherent hopping, solid lines to the coherent superexchange, and dot−dashed lines to the partially coherent hopping. The sum of all three net flux ratios is unity, as in eq 13. Up to the donor−bridge energy gap $20\beta^{-1}$, the incoherent hopping dominates, but the efficiency of the incoherent hopping decreases with the donor−bridge energy gap while the partially coherent hopping contribution increases. With $25\beta^{-1}$, partially coherent hopping starts to dominate over incoherent hopping.

a few charges are transported through coherent superexchange pathways. The lifetime of the coherent superexchange increases with the donor−bridge energy gap, 50 ps for $\beta E_2 = 20$ and 75 ps for $\beta E_2 = 25$. The partially coherent hopping net flux ratio exhibits a delay to enter the transport such that, in Figures 3b−d, the partially coherent hopping flux ratio increases slowly for the initial 10 ps until it reaches a steady value. Net flux ratios of the acceptor state in Figure 3 have positive values since electrons are accumulated in the acceptor state regardless of the transport type. For the net flux ratio of the donor state, negative values are possible due to electron transfer to the acceptor through specific pathways.

Figure 4 presents mean values of the net flux ratios of the acceptor population increase as a function of the donor−bridge energy gap. The time average was taken for the first 100 ps of the simulation. The incoherent hopping contributes significantly to the electron transfer even for high-energy bridges. In particular, up to $\beta E_2 = 5$, the electron transfer occurs mostly by the single mechanism of incoherent hopping with its flux ratio close to 1. As the donor−bridge energy gap becomes large, the incoherent hopping net flux ratio decreases, and at the same time, the partially coherent hopping net flux ratio increases. The coherent superexchange contribution grows very slowly so that even with a very large donor−bridge energy gap of $\beta E_2 = 15$, the coherent superexchange net flux ratio is still insignificant. It is worthy of mentioning the finite temperature effect at this point. With the positive donor−bridge energy gap (high-lying bridges), it is possible to have some population in the bridge due to the thermal activation. Incoherent hopping is then to follow from thermal activation of a specific intermediate state.[23]

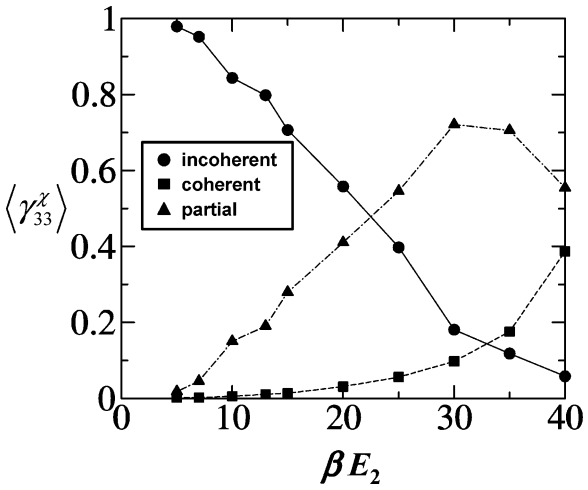

Figure 4. Mean of net flux ratios as a function of the energy gap between the donor and the bridge. The time average was taken for the first 100 ps of the simulation. The role of the donor−bridge energy gap is illustrated; the governing transport mechanism shifts from incoherent hopping to partially coherent hopping where the donor−bridge energy gap is about $22\beta^{-1}$ and eventually shifts to coherent superexchange. Note that lines are drawn to guide the eye.

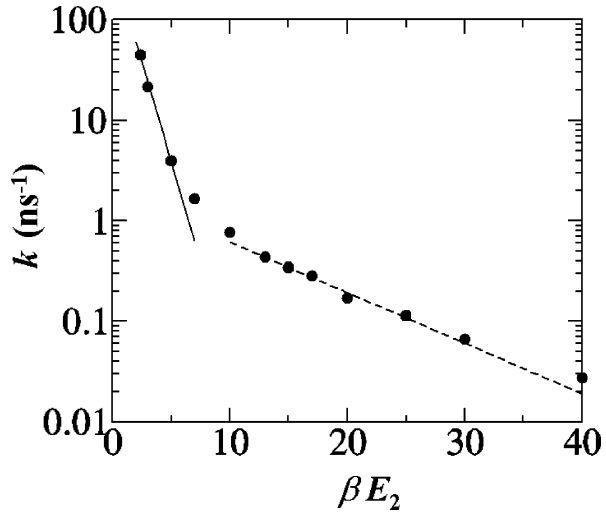

Figure 5. Transfer rate constants of the acceptor electronic population increase as a function of the energy gap between the donor and the bridge; circles are for the three-state model in eq 12, and triangles are for the two-state model where the donor and acceptor coupling constants are chosen using a McConnell form of the product.[13] The electron transfer becomes slower with the donor−bridge energy gap as anticipated. The solid and the dashed lines are exponential fits of three-state time constants for the donor−bridge energy gap $2.4\beta^{-1}-7\beta^{-1}$ and $13\beta^{-1}-40\beta^{-1}$, respectively.

However, the incoherent flux ratio decreases much more slowly than the exponential decay of the thermally activated population. Thus, the incoherent hopping dominance is not fully accounted for by thermal activation alone. With $\beta E_2 > 30$, the contribution from coherent superexchange grows substantially, and as $\langle\gamma_{33}^{p}\rangle$ decreases, $\langle\gamma_{33}^{c}\rangle$ increases.

In Figure 5, time constants of the electron population increase in the acceptor state (circles) are presented as a function of the donor−bridge energy gap. The time constants are estimated by assuming an exponential increase in the charge accumulation over time. The lines in Figure 5 are exponential fits of the time constants in two regimes, an incoherent-hopping-dominated regime for the donor−bridge energy gap $\beta E_2 = 2.4-7$ and a combination of the incoherent hopping, partially coherent hopping, and coherent superexchange regimes for the donor−bridge energy gap $\beta E_2 = 13-40$. When incoherent hopping governs the transport, it is clearly visible that the transfer rate constant decreases exponentially with the donor−bridge energy gap. The triangles in Figure 5 are the time constants obtained from a two-state model in which a bridge state is ignored and the coupling constant between a donor and an acceptor is determined according to the McConnell form of the product $V_{12}V_{23}/E_2$.[13] The rest of the parameters are maintained the same as those of the three-state model.The path integral method discussed in section 2 is used for a 2×2 matrix form of eq 12. Since the coupling strength, V_{12} and V_{23} in eq 12 are unchanged with the donor−bridge energy gap, the effective superexchange coupling constant decreases as an inverse of the donor−bridge energy gap. The three-state transfer rate constants agree well with the two-state transfer rate constants in $10 \le \beta E_2 < 40$ while the two-state model predicts slower electron transfer in $\beta E_2 < 10$. If the overall electron transfer in the three-state model is governed by the coherent superexchange mechanism, then the two models should agree over the entire range of the donor−bridge energy gap. In Figure 5, however, the two rates disagree where $\beta E_2 < 10$, indicating that mechanisms other than the coherent superexchange play an important role in such configurations. This observation also agrees well with the findings in Figure 4, in which the incoherent hopping contribution is greater than 75% of the overall contribution.

4. Concluding Remarks

This paper investigated the effect of the donor−bridge energy gap on the electron-transfer mechanism, an essential issue in understanding the dynamics of electronic devices and systems whose function is characterized by their electronic conductance. In particular, the system of interest is the reaction center of the photosynthetic purple bacteria, which consists of a simple donor−bridge−acceptor triad linearly coupled to a dissipative bath.The electron-transfer mechanism was examined as a function of the donor−bridge energy gap between a donor and a bridge while the electronic coupling strength between the states and the donor−acceptor energy gap was maintained as a constant. Accurate real-time quantum mechanical simulations of the time evolution of the charge accumulation on reduced electronic states were performed using a recently developed OFPF path integral method in which the relative contributions of incoherent hopping, coherent superexchange, and partially coherent hopping mechanisms were evaluated by separating pathways that belong to a specific mechanism. It was proven that the donor−bridge energy gap plays an important role in determining the governing electron-transfer mechanism. We observed a smooth and slow transition of the electron-transfer mechanism from incoherent hopping to partially coherent hopping and eventually to coherent superexchange, according to the donor−bridge energy gap. In addition, the three mechanisms were found to coexist for a wide range of the donor−bridge energy gaps. It has also been shown that the incoherent hopping and the coherent superexchange do not exclude each other; only an extremely high bridge-state energy can exclude incoherent hopping processes.

It should be noted that the modified OFPF path integral method provided an efficient simulation tool, which can accurately evaluate the relative transfer efficiency of each mechanism, the incoherent hopping, the coherent superexchange, and the partially coherent hopping as an intermediate transfer mechanism. It is obvious that not only the donor−bridge energy gap controls the mechanism but also the coordination of the donor−bridge energy gap between the states, the electronic coupling constants, and the number of bridges. Although path integral studies of large systems, for example, long-range electron-transfer systems with a large number of bridges and slow baths, are challenging due to an exponential increase in the required computational effort, further investigations related to these issues will greatly influence the development and the design of molecular electronic devices and systems.

Acknowledgment. This work was supported by the KOSEF (Korea Science and Engineering Foundation) through Grant No. R04-2004-000-10009-0.

References and Notes

(1) Kubatkin, S.; Danilov, A.; Hjort, M.; Cornil, J.; Brédas, J.-L.; Stuhr-Hansen, N.; Hedegård, P.; Bjørnholm, T. *Nature* **2003**, *425*, 698.

(2) Nitzan, A.; Ratner, M. A. *Science* **2003**, *300*, 1384.

(3) Osyczka, A.; Moser, C. C.; Daldal, F.; Dutton, P. L. *Nature* **2004**, *427*, 607.

(4) Segal, D.; Nitzan, A.; Davis, W. B.; Wasielewski, M. R.; Ratner, M. A. *J. Phys. Chem. B* **2000**, *104*, 3817.

(5) Giese, B. Amaudrut, J. Köhler, A.-K.; Spormann, M.; Wessely, S. *Nature* **2001**, *412*, 318.

(6) Tung, G. S. M.; Kurnikov, I. V.; Beratan, D. N. *J. Phys. Chem. B* **2002**, *106*, 2381.

(7) Jortner, J.; Bixon, M.; Voityuk, A. A.; Rösch, N. *J. Phys. Chem. A* **2002**, *106*, 7599.

(8) Sim, E. *J. Phys. Chem. B* **2004**, *108*, 19093.
(9) Petrov, E. G.; May, V. *J. Phys. Chem. A* **2001**, *105*, 10176.
(10) Weiss, E. A.; Ahrens, M. J.; Sinks, L. E.; Gusev, A. V.; Ratner, M. A.; Wasielewski, M. R. *J. Am. Chem. Soc*. **2004**, *126*, 5577.
(11) Sim, E. *J. Chem. Phys*. **2001**, *115*, 4450.
(12) Beratan, D. N.; Onuchic, J. N.; Winkler, J. R.; Gray, H. B. *Science* **1983**, *258*, 1740.
(13) McConnell, H. M. *J. Chem. Phys*. **1961**, *35*, 508.
(14) Feynman, R. P.; Vernon, F. L. *Ann. Phys*. **1963**, *24*, 118.
(15) Makri, N.; Makarov, D. E. *J. Chem. Phys*. **1995**, *102*, 4600. Makri, N.; Makarov, D. E. *J. Chem. Phys*. **1995**, *102*,*102*, 4611.
(16) Sim, E.; Makri, N. *Chem. Phys. Lett*. **1996**, *249*, 224.
(17) Leggett, A. J.; Charcravarty, S.; Dorsey, A. T.; Fisher, M. P. A.; Garg, A.; Zwerger, W. *Rev. Mod. Phys*. **1987**, *59*, 1.
(18) Makri, N. *J. Phys. Chem*. **1999**, *103*, 2823.
(19) Sim, E.; Makri, N. *Comput. Phys. Commun*. **1997**, *99*, 335.
(20) Heller, B. A.; Holten, D.; Kirmaier, C. *Science* **1995**, *269*, 940.
(21) Makri, N.; Sim, E.; Makarov, D. E.; Topaler, M. *Proc. Natl. Acad. Sci. U.S.A.* **1996**, *93*, 3926.
(22) Sim, E.; Makri, N. *J. Phys. Chem. B* **1997**, *101*, 5446.
(23) Petrov, E. G.; Zelinskyy, Y. R.; May, V. *J. Phys. Chem. B* **2004**, *108*, 13208.